JOURNAL OF GEOPHYSICAL RESEARCH, VOL. 106, NO. D14, PAGES 15,345–15,355, JULY 27, 2001

Applications of SHEBA/FIRE data to evaluation of snow/ice albedo parameterizations

J. A. Curry and J. L. Schramm

Program in Atmospheric and Oceanic Sciences, Department of Aerospace Engineering Sciences, University of Colorado, Boulder

D. K. Perovich

U.S. Army Cold Regions Research and Engineering Laboratory, Hanover, New Hampshire

J. O. Pinto

Program in Atmospheric and Oceanic Sciences, Department of Aerospace Engineering Sciences, University of Colorado, Boulder

Abstract. Climate models use a wide variety of parameterizations for surface albedos of the ice-covered ocean. These range from simple broadband albedo parameterizations that distinguish among snow-covered and bare ice to more sophisticated parameterizations that include dependence on ice and snow depth, solar zenith angle, and spectral resolution. Several sophisticated parameterizations have also been developed for thermodynamic sea ice models that additionally include dependence on ice and snow age, and melt pond characteristics. Observations obtained in the Arctic Ocean during 1997-1998 in conjunction with the Surface Heat Budget of the Arctic Ocean (SHEBA) and FIRE Arctic Clouds Experiment provide a unique data set against which to evaluate parameterizations of sea ice surface albedo. We apply eight different surface albedo parameterizations to the SHEBA/FIRE data set and evaluate the parameterized albedos against the observed albedos. Results show that these parameterizations yield very different representations of the annual cycle of sea ice albedo. The importance of details and functional relationships of the albedo parameterizations is assessed by incorporating into a single-column sea ice model two different albedo parameterizations, one complex and one simple, that have the same annually averaged surface albedo. The baseline sea ice characteristics and strength of the ice-albedo feedback are compared for the simulations of the different surface albedos.

1. Introduction

The correct determination of sea ice albedo in climate models is essential for proper treatment of the ice-albedo feedback and related cryospheric processes in climate models. The ice-albedo feedback mechanism is described as follows: As temperatures increase, the extent of snow and ice is reduced, decreasing the surface albedo and increasing the amount of sunlight that is absorbed by the Earth-atmosphere system. Conversely, a temperature decrease will increase the surface albedo and thus reinforce the cooling. *Curry et al.* [1995] further considered the impact of internal sea ice processes (e.g., formation of melt ponds, aging of sea ice) on the ice-albedo feedback mechanism. The ice-albedo feedback has been a particular subject of discussion in the context of greenhouse warming [e.g., *Spelman and Manabe*, 1984; *Dickinson et al.*, 1987; *Washington and Meehl*, 1986; *Ingram et al.*, 1989]. Atmospheric models with doubled CO_2 concentrations have found that the warming is considerably amplified in the Arctic [e.g., (*IPCC*), 1990]. Most model projections of amplified polar warming are associated with a substantial retreat of sea ice, in some cases the summertime arctic sea ice completely disappears. The predicted warming in the high latitudes has been at least partly attributed to the ice-albedo feedback mechanism.

The albedo of a surface is defined as the ratio of the solar energy reflected by the surface to that incident upon it. The spectrally integrated value is a function of surface characteristics, solar zenith angle, and atmospheric properties, including cloudiness. The optical properties of a snow or ice cover which determine its albedo are the coefficients of spectral absorption and scattering and the associated phase function of single scattering [e.g., *Maykut et al.*, 1992]. Snow and ice are transparent in the visible region and moderately absorptive in the near infrared. As described by *Grenfell and Maykut* [1977] and *Grenfell and Perovich* [1984] from field observations, snow optical properties depend on grain size and shape, depth of the snow layer and optical properties of the underlying surface, surface roughness, liquid water content, and any impurities. Sea ice optical properties depend on ice thickness, brine and air bubbles in the ice, and surface conditions, such as an ice crust on the surface, frost flowers on young ice, or melt ponds [*Perovich*, 1996]. The albedo of dry snow has a specular component and hence depends on solar zenith angle. The effect of clouds on incoming solar radiation is to change the spectral distribution and to alter the zenith angle of the radiation inci-

Paper number 2000JD900311.
0148-0227/01/2000JD900311$09.00

dent on the surface. The net effect of overcast skies on the spectrally averaged albedo of snow and ice surfaces is to increase the albedo.

A diversity of ice and snow albedo schemes are used in climate models and uncoupled sea ice models (for a review, see *Barry*, [1996], also section 3 of this paper). Most parameterizations are very simple, depending on surface type (ice, snow, or open water) and surface temperature. A few parameterizations include snow depth and ice thickness and consideration of melting snow. Fewer still include spectral dependence (visible versus near infrared) and zenith angle dependence. These prescribed albedos are usually based on limited data from site-specific case studies or are subjectively chosen. In some instances, modelers tune their albedo formulations to give a good control simulation. For example, *Manabe and Stouffer* [1980] used unrealistically low albedos to offset the model's neglect of ocean transports. Some modelers use artificially high melting surface albedos to prevent ice thicknesses which are too small [e.g., *Hibler*, 1980]. Such tuning can have undesirable consequences. In uncoupled models, tuning of the sea ice albedo may conceal serious errors in the model formulation. In coupled models, tuning of the albedo has considerable effects on model climate sensitivity [e.g., *Washington and Meehl*, 1986]. For climate simulations, it is not sufficient to have a correct surface albedo and sea ice mass balance for the control simulation, but the correct physical dependencies must be included so that the sea ice albedo feedback mechanism and its interaction with other feedbacks is correctly simulated. In coupled models, a summertime surface albedo that is too high can give the wrong sign of the cloud-radiative forcing [*Curry et al.*, 1996].

More sophisticated surface albedo schemes are available [e.g., *Schramm et al.*, 1997; *Flato and Brown*, 1996]. The Schramm et al. scheme has synthesized a variety of observational and modeling results into a surface albedo parameterization that considers both the spectral variation in albedo and its dependence on solar zenith angle. Five surface types are included, many of which can be present in a single grid cell at a given time step: new snow, melting snow, bare ice, meltwater ponds, and open water, for each of the four intervals in the solar spectrum. Because this scheme depends on surface features that are not easy to simulate (e.g., melt ponds) and cloud properties, errors in other components of the model may lead to a less realistic control simulation than a cruder albedo parameterization scheme. However, it is precisely these functional albedo dependencies that are necessary to simulate the correct ice albedo feedback.

Climate modelers have justified using simple parameterizations based on the lack of observations against which to evaluate them. Some limited comparisons of modeled versus observed surface albedos have been conducted using satellite estimates [e.g., *Ross and Walsh*, 1987]. Several satellite analyses of arctic surface albedo have been prepared [e.g., *Rossow et al.*, 1989; *Lindsay and Rothrock*, 1994]. Uncertainties in the satellite-derived surface albedos are associated with cloud thresholding, aerosols, ozone, and water vapor. Since these analyses are made for only clear sky pixels, the albedo values are biased low relative to all-sky values. Although these satellite-derived surface albedo data sets have some significant errors, they are still of some use in evaluating the performance of climate models. However, comparing modeled to satellite-derived fields is not sufficient to evaluate the surface albedo parameterization. For example, a perfectly accurate sea ice albedo parameterization may be used, but if the model is producing a sea ice field that is substantially in error, then the simulated albedo will be in error.

The Surface Heat Budget of the Arctic Ocean (SHEBA) [*Perovich et al.*, 1999] and FIRE Arctic Clouds Experiment [*Curry et al.*, 2000] observational data set provides an excellent opportunity to evaluate parameterizations of sea ice albedo. This experiment, described in section 2, provides comprehensive surface albedo measurements of a multiyear ice floe over an entire annual cycle. In addition to surface albedo measurements, observations were made of all the parameters required as input values to the diverse sea ice albedo parameterizations. Furthermore, a complete set of observations of surface fluxes, sea ice mass balance, and ice floe dynamics was obtained, which can be used to force and evaluate a one-dimensional sea ice model.

In this paper we use the SHEBA data to evaluate a variety of sea ice albedo parameterizations that are used in climate models and uncoupled sea ice models. The seasonal cycle of the albedo parameterizations is evaluated specifically for the winter period of fresh and dry snow, the late spring period of snowmelt, the summer melt season, and the autumnal period of freezing. The importance of details and functional relationships of the albedo parameterizations is assessed by incorporating into a single-column sea ice model two different albedo parameterizations, one complex and one simple, which have the same annually averaged surface albedo. The baseline sea ice characteristics and strength of the ice-albedo feedback are compared for the simulations of the different surface albedos.

2. Data

The data used to evaluate the surface albedo parameterizations are obtained from the Surface Heat Budget of the Arctic Ocean (SHEBA) project [*Perovich et al.*, 1999] and the FIRE Arctic Clouds Experiment [*Curry et al.*, 2000]. The SHEBA observations were made during the period October 30, 1997 through October 10, 998. The Canadian Coastguard ice breaker *Des Groseilliers* was deployed in a multiyear ice floe at 75°16.3'N, 142° 41.2' W. Over the course of the field study, the SHEBA ice camp drifted considerably northwestward, reaching 80°N 162°W by the end of the experiment. The FIRE Arctic Clouds Experiment included aircraft overflights of the SHEBA ice camp during April 8 through July 28, 1998.

A variety of measurements of the atmosphere, sea ice, and upper ocean were made during SHEBA and the FIRE Arctic Clouds Experiment [*Perovich et al.*, 1999; *Curry et al.*, 2000]. Here we focus specifically on observations of surface albedo and also the meteorological and surface parameters that are used as inputs to surface albedo parameterizations for multiyear sea ice: surface skin temperature, surface air temperature, snow depth, ice thickness, melt pond fraction, and melt pond depth.

2.1. Instrumentation

Measurements were made of wavelength-integrated and spectral values of surface albedo, using Kipp and Zonen radiometers that integrate over wavelength from 300 to 2800 nm. These values are accurate to within 0.01. Spectral albedos from 400 to 2000 nm were also measured using a Spectron Engineering SE-590 spectroradiometer. Albedo measurements were made at least weekly from April to October and every other day from June to August. Measurements were made every 2.5 m

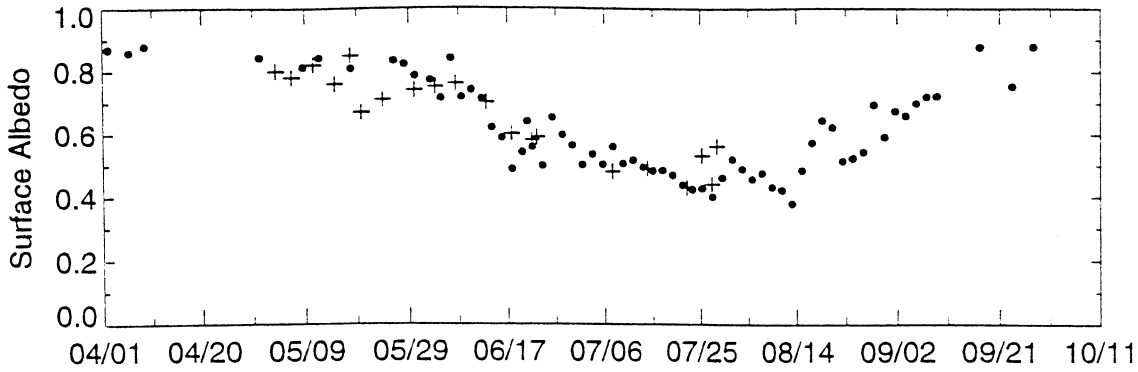

Figure 1. Observations of surface albedo obtained at the SHEBA ice station. Circles, surface measurements along the 500-m albedo line; pluses, values obtained from the C130 aircraft.

along a 200-m-long albedo line that encompassed different snow and ice conditions over the heterogenous sea ice cover of the multiyear ice floe. The values for each day were used to compute an areally averaged albedo.

In addition to the surface-based measurements, observations of surface albedo were made from the NCAR C-130 research aircraft using the Radiation Measurement System (RAMS) [*Pope et al.*, 2000], which includes uplooking and downlooking multichannel radiometers that have a hemispheric field of view and seven channels from the ultraviolet to the near infrared (0.2-3.9 _m). The aircraft observations covered a region of 20 x 20 km, centered on the SHEBA ice camp.

Ice thickness was measured using ablation stakes and thickness gauges at more than 100 different locations on the ice floe. The gauges were manually read every other day from June to August and approximately weekly the remainder of the year. Vertical profiles of ice temperatures were automatically recorded every hour throughout the experiment at seven sites [*Perovich et al.*, 1999]. Snow depth was measured every 1-5 m along the main 500-m survey line either manually using a graduated ski pole or a magnaprobe [*Perovich et al.*, 1999]. Manual measurements were rounded off to the nearest centimeter, and magnaprobe values were accurate to within 0.5 cm. Snow depths were averaged along the survey line. Measurements were made every 1-2 weeks from October to May and every other day from June to August.

Melt pond characteristics (pond fraction and pond depth) were measured along the albedo line. During July, statistics on melt pond fraction were also obtained from the C-130 video camera [*Tschudi et al.*, 2000]. The surface-based melt pond analysis covered the 200-m-long line, while the aircraft analysis covered an area of 20 x 20 km. During the later part of July the surface-based melt pond fraction exceeded the aircraft value, most probably a result of small-scale variability in pond coverage.

Surface skin temperature was measured using a broadband Eppley radiometer and assuming a surface emissivity of 0.99 [*Claffey et al.*, 1999]. Measurements were made every 10 s, and hourly averaged values are used in this study. Comparison of several different methods of determining surface skin temperature suggests an uncertainty in the surface temperature of about 1°C. Air temperature was measured using Vaisala temperature sensors at various levels in the atmosphere; the value used here has been interpolated to 10 m. Air temperature measurements are accurate to within about 0.1 °C.

2.2. Description of Observations

The annual cycle of surface albedo is shown in Figure 1. Observations are presented from surface measurements obtained from the albedo line and from the C-130 aircraft; the slightly lower values obtained from the C-130 aircraft reflect contributions from thin ice and leads. During April and May, when the surface consists of dry snow, surface albedo averaged 0.84. The melt season lasted a total of 80 days from late May to mid-August. During the first two weeks of June when most of the snowmelt occurred, the average surface albedo was 0.77. Melt ponds formed in early June and continued to develop into August. The surface albedo decreased throughout the summer melt season and reached a minimum value of 0.38 on August 12. Beginning on August 12, the melt ponds began to freeze, causing the albedo to increase. Snow began to accumulate on the ice in late August and by mid-September the snow cover was roughly 10 cm deep. The albedo began to increase, reaching its winter-spring value by the end of September.

The annual cycle of surface conditions at SHEBA are described by *Perovich et al.* [1999]. The thickness of the undeformed multiyear ice at deployment was 1.7-2.0 m. The ice grew 75 cm during winter and melted 110 cm during the summer melt season. Snow depth increased quickly in the fall and more slowly through the winter, reaching an average depth of 34 cm in the spring. The first rainfall of the season on May 29 heralded the onset of snowmelt. Most of the snow cover melted in just a few weeks, with a few small, scattered snowdrifts lasting until mid-July. There were occasional snow flurries during summer, but it was not until late August that snow began to accumulate on the surface.

Melt ponds formed in June as the snow melted, then deepened and grew in horizontal extent during June through mid-August. Along the albedo line, ponds covered 38% of the surface area during the peak of the melt season and reached an average depth of 39 cm.

Surface skin and air temperatures are shown in Figure 2. When compared with climatology, SHEBA was relatively cool during winter and warm during spring. The onset of summer melt (May 29) is reflected by surface temperature reaching 0°C. During the summer melt period the surface temperature oscillates slightly around the melting point but, accounting for the error of the measurements, appears to remain at the melting temperature during this period except for during a clear period on July 17.

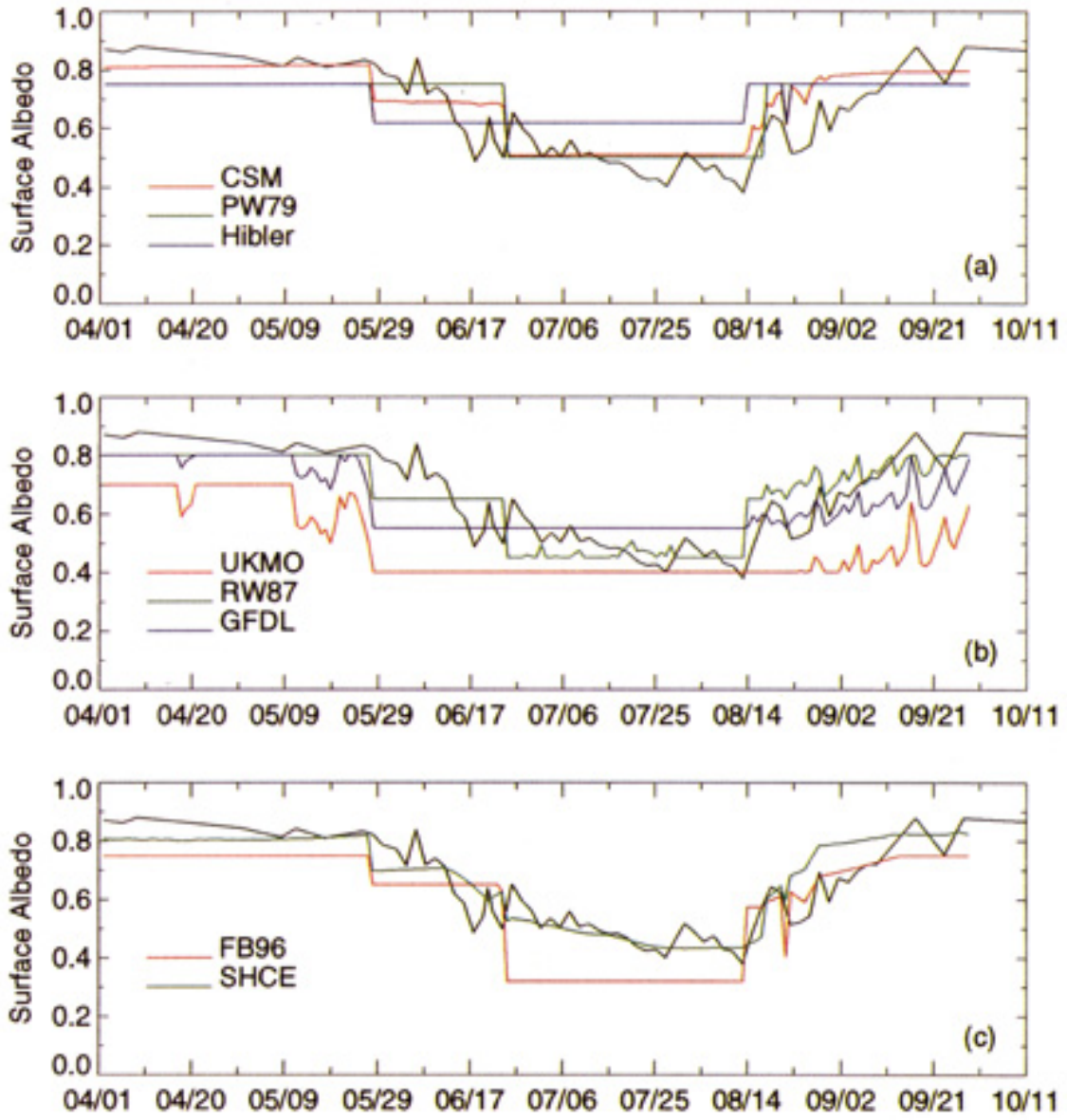

Plate 1. Comparison of parameterized versus observed surface albedos. Parameterized albedo values were determined using SHEBA observations as input. Solid black line represents the observed albedo and colored lines the parameterized albedos. (a) NCAR CCM3 [*Briegleb and Bromwich,* 1998; PW79 *Parkinson and Washington,* 1979; *Hibler,* 1980], (b)UKMO [*Ingram et al.,* 1989; *Ross and Walsh,* 1987], GFDL [*Manabe et al.,* 1992], (c)*Flato and Brown* [1996] and *Schramm et al.* [1997].

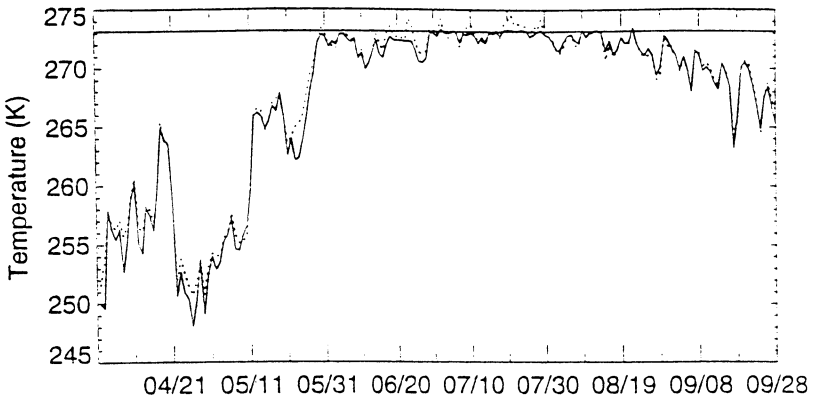

Figure 2. Observations of surface temperature obtained from the meterological tower at the SHEBA ice station. Solid cuve, surface skin temperature; dashed, surface air temperature (10 m).

3. Albedo Parameterizations

In this section we focus on the albedos observed along the 200-m survey line over multiyear sea ice, during the period April to October. The albedo parameterizations chosen for this study aim to represent the spectrum of parameterizations used in general circulation models (GCMs), regional models of the Arctic basin, and uncoupled sea ice models.

3.1. Parameterization Descriptions

The simplest of the surface albedo parameterizations considers only broadband values of surface albedos for two different surface types: snow and bare ice. A model that parameterizes the albedo in this fashion is the large-scale sea ice model of *Parkinson and Washington* [1979] (hereafter referred to as PW79). The snow and ice albedos in PW79 are 0.75 and 0.50, respectively.

The basin-scale sea ice model of *Hibler* [1980] does not include snow cover explicitly but included an albedo that varied with surface temperature. The surface albedo is 0.75 when the surface temperature was below freezing, identical to the snow albedo of PW79. When the surface temperature is equal to the freezing point of 273.15 K, the ice albedo is set to 0.616.

The United Kingdom Meteorological Office (UKMO) GCM, as described by *Ingram et al.*, [1989] model, includes a surface albedo parameterization that depends on the simulated surface skin temperature T_s:

$$\alpha = \begin{cases} 0.7 & \text{if } T_s \le 261.2\ \text{K} \\ 0.7 - 0.03(T_s - 261.2) & \text{if } 261.2\ \text{K} < T_s < 271.2\ \text{K} \\ 0.4 & \text{if } T_s = 271.2\ \text{K} \end{cases} \quad (1)$$

This parameterization includes a simple representation of the effects of surface warming on the albedo. The linear dependence of albedo on surface temperature over a 10°C range attempts to capture the effects of snow aging. The low albedo when the surface temperature is at the melting point simulates the effects of melt ponds.

Ross and Walsh [1987] also use a parameterization that decreases the albedo linearly with temperature when the temperature approaches the freezing point. Separate snow (subscript s) and ice (subscript *i*) albedos are included which depend on surface and air temperature, respectively, as follows

$$\alpha_s = \begin{cases} 0.80 & \text{if } T_s < 268\ \text{K} \\ 0.65 - 0.03T_s & \text{if } 268\ \text{K} < T_s < 273\ \text{K} \\ 0.65 & \text{if } T_s = 273\ \text{K} \end{cases}$$

$$\alpha_i = \begin{cases} 0.65 & \text{if } T_s < 273\ \text{K} \\ 0.45 + 0.04T_a & \text{if } 273\ \text{K} < T_a < 278\ \text{K} \\ 0.45 & \text{if } T_a = 278\ \text{K} \end{cases} \quad (2)$$

where T_a is the air temperature in degrees Celsius. Since the surface temperature is constrained not to exceed the melting point, air temperature is used in this parameterization to allow the ice albedo to decrease below that of melting snow.

The parameterization used in the GFDL climate model [*Manabe et al.*, 1992] includes, in addition to a dependence on surface skin temperature, variations associated with ice depth:

$$\alpha = \begin{cases} \alpha^* & \text{if } h \ge 1\ \text{m} \\ \sqrt{h}(\alpha^* - \alpha_o) + \alpha_o & \text{if } h < 1\ \text{m} \end{cases}$$

where

$$\alpha^* = \begin{cases} \alpha_i & \text{if } T_s \ge T_m \\ \alpha_i + 0.025(T_m - T_s) & \text{if } (T_m - 10\ \text{K}) < T_s < T_m \\ \alpha_s & \text{if } T_s \le (T_m - 10\ \text{K}) \end{cases} \quad (3)$$

where T_m is the melting temperature and the subscript "zero" refers to ocean.

Flato and Brown [1996] developed a surface albedo parameterization for landfast ice, which we believe has general applicability for sea ice and climate models:

$$\alpha = \begin{cases} \alpha_o & \text{if } h_i < h_{\min} \\ \min\left[\alpha_s, \alpha_i + h_s(\alpha_s - \alpha_i)/c_{10}\right] & \text{if } h_i \ge h_{\min} \text{ and } h_s \le c_{10} \\ \alpha_s & \text{if } h_i \ge h_{\min} \text{ and } h_s > c_{10} \end{cases}$$

$$\alpha_i = \begin{cases} \max\left(\alpha_o, c_{11} h_i^{0.28} + 0.08\right) & \text{if } T < T_m \\ \min\left(\alpha_{mi}, c_{12} h_i^2 + \alpha_o\right) & \text{if } T = T_m \end{cases}$$

$$\alpha_s = \begin{cases} 0.75 & \text{if } T < T_m \\ 0.65 & \text{if } T = T_m \end{cases} \quad (4)$$

where $c_{11} = 0.55\ m^{-0.28}$, $c_{12}=0.075\ m^{-2}$, $\__{mi} = 0.55$ is the melting ice albedo and $\__o$ is the open water albedo, equal to 0.15, c_{10} is 0.1 m, and h_{min} is 0.001 m.

A modified version of the NCAR CSM1.3 parameterization includes visible and near-infrared albedos (B. Briegleb, personal communication, 2000). This parameterization includes thin, thick, and melting ice as well as dry and wet snow. Thin ice is defined as that 0.5 m thick or less. The ice albedo is defined as

$$\alpha_i(\text{vis}) = \begin{cases} 0.48 + 0.88(h_i - 0.25) & h_i \le 0.5\,m \\ 0.70 & h_i > 0.5\,m \end{cases}$$
$$\alpha_i(\text{nir}) = \begin{cases} 0.28 + 0.88(h_i - 0.25) & h_i \le 0.5\,m \\ 0.50 & h_i > 0.5\,m \end{cases} \quad (5)$$

The criteria for melting ice is a surface temperature equal to or greater than –1°C, and the albedo is defined as

$$\alpha_m(\text{vis}) = \alpha_i(\text{vis}) - 0.10(T_s + 1.0)$$
$$\alpha_m(\text{nir}) = \alpha_i(\text{nir}) - 0.10(T_s + 1.0) \quad (6)$$

The visible and near-infrared albedos of dry snow are 0.95 and 0.70, respectively. Wet snow exists when the surface temperature is equal to or greater than –0.3°C with visible and near-infrared albedos of 0.85 and 0.55, respectively. When a snow cover is present, the snow and ice albedos are weighted by a fractional coverage equal to $h_s/(h_s+0.02)$, where the snow depth is in liquid water equivalent.

The parameterization developed by *Schramm et al.* [1997, (hereinafter referred to as SHCE)] is described in Table 1. The SHCE scheme considers both the spectral variation in albedo and its dependence on solar zenith angle. Five surface types are included, many of which can be present in a single grid cell at a given time step: new snow, melting snow, bare ice, meltwater ponds, and open water, for each of four intervals in the solar spectrum. The parameterization of snow and bare ice albedo depend on snow and ice thickness. The net albedo is determined from a weighted average of the different surface types present in the model grid cell.

3.2. Comparison With Observations

The seasonal cycle of surface albedo over multiyear ice is determined using the above parameterizations and the data described in section 2 as input. Surface albedos measured from the albedo line over multiyear ice are used in the comparison. The albedo calculated using the SHEBA conditions is indicative of what each of these models would determine for the multiyear sea ice present in the grid cell; no attempt is made here to account for the influence of leads on the grid-cell sea ice albedo.

Table 1. Spectral Albedos for Five Surface Types Included in the Work of *Schramm et al.* [1997 (SHCE)]

Surface Type	Band 1 0.25-0.69 μm	Band 2 0.69-1.19 μm	Band 3 1.19-2.38 μm	Band 4 2.38-4.00 μm
Dry snow, α_s				
direct	0.980-0.008μ_o	0.902-0.116μ_o	0.384-0.222μ_o	0.053-0.047μ_o
diffuse	0.975 linearly reduced to bare ice value if h_s<0.1 m	0.832 linearly reduced to bare ice value if h_s<0.1 m	0.250 linearly reduced to bare ice value if h_s<0.1 m	0.025 linearly reduced to bare ice value if h_s<0.1 m
Melting snow, α_{ms}				
$h_s \ge 0.1$ m	0.871 linearly reduced to bare ice value if h_s<0.1 m	0.702	0.079	0.010
Bare MY ice	0.778	0.443	0.055	0.036
Bare FY ice, α_{fy}				
$0<h_i<1$ m	0.760+0.140*ln(h_i)	0.247+0.029*ln(h_i)	0.55	0.36
$h_i \ge 1$ m	0.760	0.247	0.55	0.36
Melt ponds, MY ice	0.342+exp(-20.512*h_p-0.83) if cloudy 0.342+exp(-9.0 h_p-0.999) if clear	0.020+exp(-14.187*h_p-0.860)	0.033+exp(-2.58*h_p-3.82)	0.030
Melt ponds, FY ice	0.251+exp(-17.134 h_p-0.675) if cloudy, $h_i \ge 1$ 0.25+exp(-17.134h_p)(α_{fy}-0.251) if cloudy, h_i<1 0.251+exp(-11.0 h_p-1.174) if clear	0.01+exp(-17.31 h_p-1.439) if $h_i \ge 1$ 0.01+exp(-17.31 h_p) (α_{fy}-0.01) if h_i<1	0.033+exp(-2.28 h_p-3.82)	0.030
Open water				
Direct, α_{wr}	α_w + 0.0082	α_w - 0.0070	α_w - 0.0070	α_{wr} - 0.0070
Diffuse, α_{wf}	0.060	0.060	0.060	0.060

Here $\mu_o = \cos\theta_o$, where θ_o is the zenith angle in degrees, h_i is ice thickness in meters, h_p is pond depth in meters, and $\alpha_w^* = 0.026/(\mu_o^{1.7} + 0.065) + 0.015(\mu_o - 0.1)(\mu_o - 0.5)(\mu_o - 1.0)$.

Table 2. Comparison of Parameterized Albedos Averaged Over an Entire Melt Cycle and Over Various Surface Types With Observed SHEBA Values

Parameterization	Seasonal Cycle JD 91-270	Dry Snow JD 91-146	Melting Snow JD 147-161	Ponded Ice JD 162-224	Fall Freeze-Up JD 225-270
Observed	0.66	0.84	0.77	0.51	0.66
CSM	0.69	0.81	0.69	0.54	0.75
PW79	0. 68	0.75	0.75	0.55	0.73
Hibler	0.69	0.75	0.62	0.62	0.75
UKMO	0.49	0.66	0.40	0.40	0.45
RW87	0.66	0.80	0.65	0.50	0.73
GFDL	0.64	0.78	0.55	0.55	0.63
FB96	0.60	0.75	0.65	0.39	0.68
SHCE	0.68	0.82	0.70	0.50	0.74

During the summer melt season, the input skin surface temperature is set to the melting point. This eliminates spurious "freezing" albedos determined from skin temperature values that drop below freezing during the summer melt period (although it appears that the freezing on July 17 was real). Also, the date of snow disappearance is set to June 24, which is the date that most of the ice is snow free (although a few pockets of snow remain until mid-July). Plate 1 and Table 2 show comparisons with observations of the annual cycle of surface albedo determined using the eight different parameterizations.

The two simplest albedo parameterizations are shown in Plate 1 (PW79, Hibler). PW79 and Hibler underestimate the dry snow albedo by 9%. The PW79 bare ice albedo is specified 0.5, which agrees well with the averaged observed albedo during the summer melt (ponded ice) period. However, since the PW79 parameterization is tied to the presence of snow, which remains until June 24, the parameterized albedos remain high even after summer melt has commenced, resulting in an average albedo of 0.55 during the summer melt (ponded ice) period. Hibler overestimates the summertime albedo by more than 10%. Both parameterizations overestimate the surface albedos during the autumn by 7-9%.

The albedo parameterizations shown in Figure 3b (UKMO, RW87, GFDL97) employ a linear dependence on surface and/or air temperature. The UKMO parameterization has a low bias for the entire seasonal cycle. The albedo for dry snow is too low by 18%, a rather low temperature of 261.2 K is the threshold for melting snow, and the melting ice albedo is specified to be 9% too low. The specification of a more accurate dry snow albedo of 0.8 and higher temperature of −5 °C denoting melting snow results in a more accurate snow albedo simulation by RW87. Also, the specified minimum albedo of 0.45 for melting ice and the dependence air temperature instead of the surface temperature results in a reasonable summertime ice albedo for RW87. The GFDL parameterization captures the broad picture of the summer melt season, and simulates the increase in albedo back to the dry snow value suprisingly well, although the snow albedos are somewhat too low. Both the RW87 and the GFDL parameterizations determine average albedos that are within 2% of the observations.

The albedos in Plate 1c (FB96, SHCE) and also CSM (Plate 1a) are calculated using more complex albedo parameterizations. All three of these albedo parameterizations produce reasonable seasonal cycles when compared with observations. The FB97 dry snow albedo value is 9% lower than observations and the melting sea ice albedo is 12% lower than observations. Recall however, that FB87 was designed for coastal fast ice, where the albedos may be genuinely lower than those in the central Arctic. The NCAR CSM parameterization is within 3% of observations for the dry snow and ponded ice periods but has discrepancies of 8-9% during the melting snow and fall freeze-up periods. The SHCE parameterization is within 1-2% for the dry snow and ponded ice periods, although albedos in the melting snow period are 7% too low and in the fall freeze-up periods are 8% too high when compared with observations.

The results shown in Plate 1 and Table 2 show that no single parameterization perfectly simulates the seasonal cycle of albedo variation during SHEBA. The daily-average-observed albedo at SHEBA was 0.66, and most parameterizations (PW79, RW87, GFDL, Hibler, CSM, and SHCE) came within a 3% of this value. The SHCE, RW87, and CSM parameterizations give reasonable seasonal cycles. The CSM and SHCE parameterizations for dry snow albedo were within 2% of the observations. PW79 provided the most accurate melting snow albedos, although this parameterization does not include melting snow as a surface type. The parameterizations that gave the closest melting ice albedos were RW87 and SHCE. The fall freeze-up albedo was determined most accurately by FB79.

4. Impact of Albedo Parameterizations on Simulated Ice Albedo Feedback

Correct simulation of the average surface albedo over sea ice may not be sufficient to represent the ice-albedo feedback and other cryospheric processes in climate models. To examine this issue, we use a single-cell ice thickness distribution model [*Schramm et al.*, 1997a; *Holland and Curry*, 1999] to examine the model sensitivity to two different surface albedo parameterizations. We compare the SHCE [*Schramm et al.*, 1997] with the PW79 [*Parkinson and Washington*, 1979] parameterization, which yield exactly the same average surface albedo (Table 2). Specifically, we examine the impact of the surface albedo on simulation of surface and ice characteristics during the SHEBA year. Also, the strength of the ice-albedo feedback in the model is compared for the two different surface albedo parameterizations.

The single-cell ice thickness distribution model is a Lagrangian model that responds to both thermodynamical and dynamical forcing [*Schramm et al.*, 1997; *Holland and Curry*, 1999]. The model allows for a specified number of level and ridged ice categories within the model domain. Divergent sea ice motion causes sea ice to be exported from the model domain, whereas convergent motion causes ice ridging to occur. Shearing of the ice pack causes both open water and pressure ridges

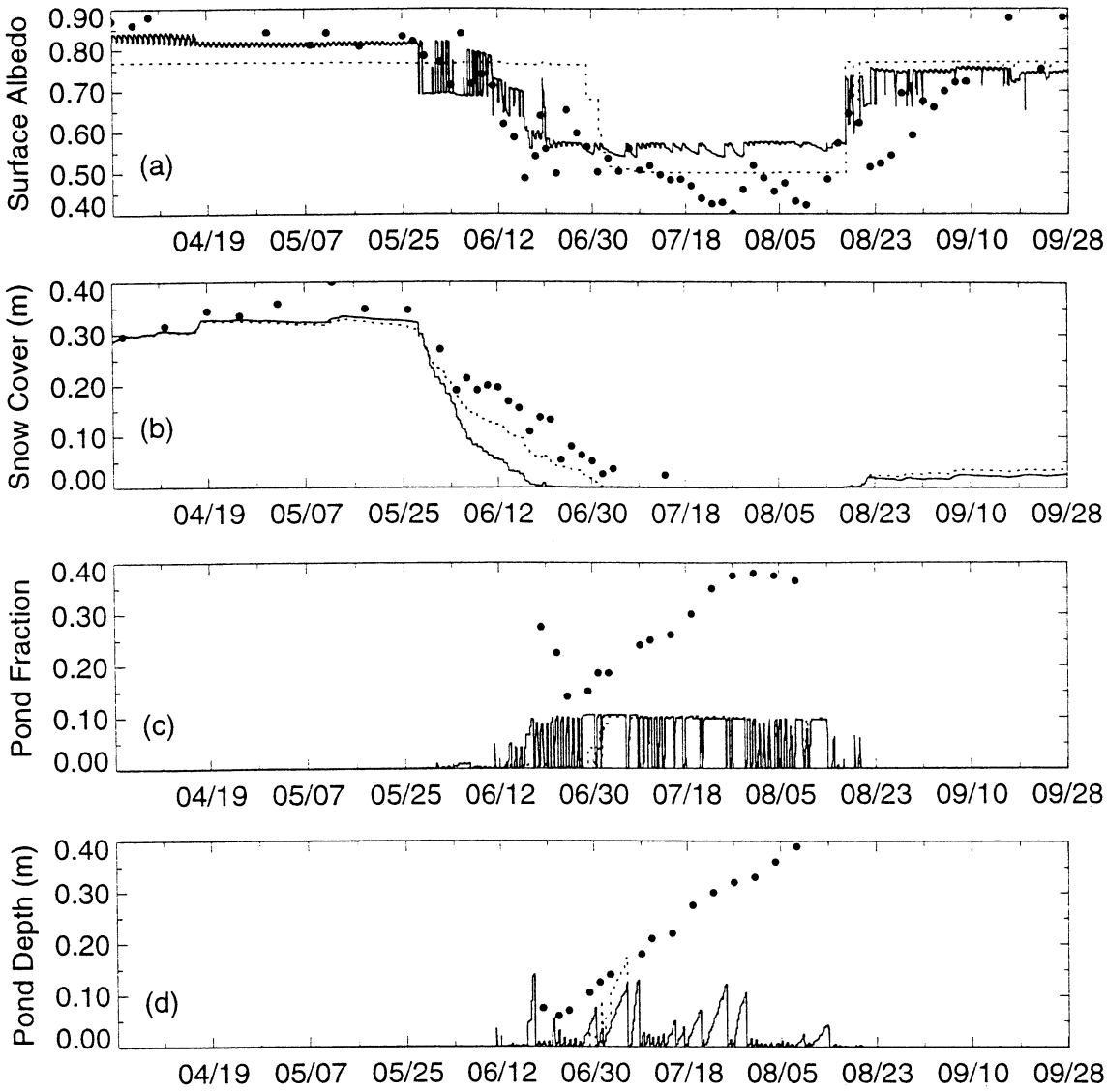

Figure 3. Comparison of the simulations with the single-cell ice thickness distribution model using the SHCE surface albedo parameterization (solid) and the PW79 surface albedo parameterization (dotted) with observations (circles). (a) Surface albedo, (b) snow depth, (c) pond fraction, (d) pond depth.

to form. Parameterization of these processes is done using a redistributior function that reorganizes the ice in the model domain based on the kinematic forcing. The different ice thickness categories are described by a variety of properties, including age, salinity, snow cover, and melt pond cover. Each ice thickness category is thermodynamically independent from one another with different interfacial heat fluxes being computed for each ice category. Spectral radiative transfer through the ice and open water is included. An explicit melt pond parameterization is included in the model, whereby a specified fraction of melt water is allowed to run off or drain into the ocean and the remainder of the water pools into melt ponds. The sea ice model is coupled to a bulk ocean mixed layer model.

4.1. Simulation of the SHEBA Annual Cycle

The single-column ice model is initialized using the ice thickness distribution determined from submarine sonar [SCICEX) (D. Rothrock, personal communication, 2000), which determined the average ice thickness of the SHEBA floe to be 1.5 m in September 1997. Then the SHEBA year is simulated using hourly surface flux data [*Andreas et al.*, 1999] and daily ice deformation determined from RADARSAT (M. Stern, personal communication, 2000). The PW79 surface albedo scheme is implemented so that the only change to the model is to the actual surface albedo parameterization itself. The full spectral radiation model is retained, although there is of course no spectral variation in the surface albedo when the PW79 parameterization is incorporated.

Figure 3a compares the simulated and observed surface albedos over multiyear ice for the SHEBA year. Because the two albedo parameterizations interact in different ways with the simulated surface features, the simulated surface albedos diverge widely particularly during the snowmelt period. The net solar radiation absorbed at the surface in the single-column cell using the two different surface albedo parameterizations are within 0.5% of each other. When compared with the seasonal cycle of albedo shown in Plate 1, it is seen that the PW79 surface albedo parameterization in the interactive model (Figure 3a) gives essentially the same values of surface albedo in the interactive model as when determined from SHEBA observa-

tions, while the SHCE parameterization gives substantially different values in the interactive model when compared with the values determined from the SHEBA data. The SHCE parameterization when used in the interactive model produces a minimum summer melt albedo of 52%, compared with a minimum value of 43% determined from using the SHEBA data as inputs. Additionally, the SHCE parameterization, when employed in the interactive model, shows a much sharper increase at the end of the melt season. This illustrates that the surface albedo parameterization with more complex dependence on surface features can give a degraded simulation of surface albedo if the simulation of surface features is deficient.

The differences between SHCE albedos determined using the SHEBA data as input versus those simulated using the single-cell ice thickness distribution model can be interpreted by comparing simulations and observations of the parameters upon which the surface albedo parameterizations for multiyear ice depend: snow depth and melt pond fraction. Comparison of the annual cycle of snow depth in Figure 3b shows that the snow melts too rapidly during spring using the SHCE parameterization. Problems with melting snow in part reflect a modeled melting snow albedo that is too low (Table 2). Figures 3c and 3d compare the simulated versus observed pond fraction and depth. The simulated pond fraction is too small and the pond depth too shallow. The problem with melt pond simulations arises from use of hourly surface heat fluxes which includes a diurnal cycle and causes ponds to freeze at night; nocturnal pond freezing was not a problem in the *Schramm et al.* [1997] calculations, which used 8-hourly forcing. The nocturnal freezing of ponds appears to be associated with not allowing ponds to warm above the freezing temperature in the simulations.

Table 3 further compares the impact of the two different surface albedo parameterizations on the simulation results. Specifically, we compare the two different simulations with observations of onset of snowmelt, amount of ice growth and ablation (top and bottom), length of melt season, lead fraction, and flux of shortwave radiation into the ocean. The two different surface albedo parameterizations give essentially the same date for onset of snowmelt and length of the melt season. However, some differences are seen in the other parameters. Because PW79 specifies a broadband albedo, while the SHCE parameterization is spectral, more shortwave radiation is transmitted to the ocean in the SHCE simulations since the visible radiation is able to penetrate the thin ice and enter the mixed layer. This results in a warmer ocean mixed layer for SHCE, which increases the lateral melting of leads (reflected by the larger maximum lead fraction for SHCE) and also the amount of basal melting. As seen from Figures 3c and 3d, simulations with the two different surface albedo parameterizations result in essentially the same simulated melt pond characteristics. However, surface ablation is higher for SHCE even though the SHCE summer melt albedo is higher than that for PW79; this is apparently associated with the earlier melting of the snow using SHCE. Although the SHCE simulation agrees better with observations than the PW79 simulation, it is assessed that the difference between the simulations using the two parameterizations is much less than the differences between either simulation and the observations.

4.2. Simulation of Ice-Albedo Feedback Mechanism

To further explore the differences between albedo parameterizations and the sea ice process which are influenced by variations in surface albedo, we examine the strength of the ice-albedo feedback mechanism for the single-cell ice thickness distribution model when each of two albedo parameterizations are included. In the context of the single-cell ice thickness distribution model, we focus on the aspect of the ice-albedo feedback mechanism associated with surface optical properties [following *Curry and Webster*, 1999].

We conduct simulations of the ice-albedo feedback in the following way [after *Curry et al.*, 1995]. Three different model simulations are required for each parameterization: (1) a baseline simulation, representing the current unperturbed climate conditions; (2) a simulation in which the climate is subject to an external perturbation, and all feedbacks are operative; and (3) a run in which the climate is subject to an external perturbation, and the ice albedo feedback mechanism is switched off by keeping the surface albedo fixed in the perturbed run to the same values used in the baseline simulation.

The feedback gain ratio R_f is then evaluated from [*Curry and Webster*, 1999]

$$R_f(T_s) = \frac{(T_s)_2 - (T_s)_1}{(T_s)_3 - (T_s)_1} \tag{7}$$

where the numerical subscripts refer to the enumerated model simulations above. As described by *Curry et al.* [1995], we also evaluate the feedback gain ratio in terms of the ice thickness h_i,

$$R_f(h_i) = \frac{(h_i)_2 - (h_{is})_1}{(h_i)_3 - (h_i)_1} \tag{8}$$

since during the summer melt, T_s does not change, but h_i does. Hence $R_f(T_s)$ is more heavily influenced by winter processes and $R_f(h_i)$ is more heavily influenced by summer processes.

Following *Curry et al.* [1995] we use a perturbation to the surface longwave radiative flux consisting of ±5 W m^{-2}. The

Table 3. Comparisons of Observations and Simulations for the SHEBA Year Using the Single-Cell Ice Thickness Distribution Mode With *Schramm et al.* (1997; (SHCE)] and *Parkinson and Washington* [1979; (PW79)] Surface Albedo Parameterizations

Parameter	SHCE	PW79	Observed
Onset of snow melt	May 28	May 28	May 26
Change in ice thickness (m)	-0.61	-0.37	(-0.35 MY)
Maximum lead fraction (%)	6.0	4.6	18
Basal ice growth (m)	0.40	0.39	0.75
Basal ablation (m)	0.25	0.24	0.40
Length of melt season (days)	71	71	80
SW transmitted to ocean (J m^{-2})	6.1x10^7	5.1x10^7	
Average July ice/ocean heat flux (W m^{-2})	7.4	5.9	
Surface ablation (m)	0.76	0.52	0.70

Table 4. Results of Perturbation Simulations Using the Single-Cell Ice Thickness Distribution Mode With *Schramm et al.* [1997; (SHCE)] and *Parkinson and Washington* [1979; (PW79)] Surface Albedo Parameterizations

Annually Averaged	Weighted Values	SHCE	PW79
Baseline	T_s(K)	256.79	256.59
	h_i(m)	3.182	3.724
+5 W m^{-2}	T_s(K)	257.34	257.10
	h_i(m)	2.504	3.604
-5 W m^{-2}	T_s(K)	256.10	256.03
	h_i(m)	3.469	4.074
Feedback Gain	Ratio		
+5 W m^{-2}	T_s(K)	1.34	1.02
	h_i(m)	3.17	1.00
-5 W m^{-2}	T_s(K)	1.50	1.04
	h_i(m)	1.39	1.07

simulations were each conducted for 30 years, with an 8-hour time step. The baseline forcing is derived from daily varying values of surface fluxes obtained from Russian ice island data. The ice deformation is determined from the AIDJEX data (the same values are used for each year).

Table 4 compares the feedback gain ratio evaluated for the simulations using the PW79 and SHCE surface albedo parameterizations, along with values of T_s and h_i for the baseline and perturbed simulations. It is seen that the baseline simulations of T_s for each of the albedo parameterizations are almost identical, although the simulation with the PW79 parameterization yields substantially thicker ice. The feedback gain ratios for PW79 are very close to unity, indicating virtually no feedback. The only mechanism in the PW79 parameterization that would produce a positive ice albedo feedback is a change in the length of the snow-free period. The feedback gain ratios for SHCE are all positive and substantially larger than the PW79 values. The value of $R_f(T_s)$ for SHCE is larger for the cooling perturbation, while the value of $R_f(h_i)$ for SHCE is very much larger for the warming perturbation. This indicates that the warming perturbation for SHCE has its greatest impact during the summer melt period, with thinner ice providing a strong positive feedback for the SHCE parameterization because of increased length of the melt season, thinning of the ice, warming of the ocean mixed layer, and enhanced surface melt.

These calculations illustrate that two different albedo parameterizations used in the same sea ice model, constrained to have the same average surface albedo and approximately the same baseline conditions, can produce substantially different strengths of the ice-albedo feedback mechanism for a warming perturbation. A more definitive comparison of the two albedo parameterizations would require a coupled atmosphere/ice model, since interactions of the surface albedo parameterization with the cloud radiation feedback may emphasize or diminish the differences between the two parameterizations.

5. Summary and Conclusions

Observations obtained in the Arctic Ocean during 1997-1998 in conjunction with the SHEBA and the FIRE Arctic Clouds Experiment are used to evaluate parameterizations of sea ice surface albedo. Eight different surface albedo parameterizations of varying complexity were selected for evaluation. Results show that these parameterizations yield very different representations of the seasonal cycle of sea ice albedo. The seasonal cycle was divided into four periods using the observed sea ice and snow characteristics: springtime snow, melting snow, melting ice, and fall freeze-up. Six of the parameterizations were within 3% of the annually averaged surface albedo, and two were within 3% of the average albedo for two periods (none of these were within 3% of the average albedo for more than two of the four periods).

The importance of the seasonal cycle of albedo and the functional relationships of the albedo parameterizations are assessed by incorporating into a single-column sea ice model two different albedo parameterizations, one complex [*Schramm et al.*, 1997; SHCE] and one simple [*Parkinson and Washington*, 1979], which have the same annually averaged surface albedo. The baseline sea ice characteristics and strength of the ice-albedo feedback are compared for the simulations of the different surface albedos. It was found that the PW79 surface albedo parameterization gives essentially the same values of surface albedo in the interactive model as when determined from SHEBA observations, while the SHCE parameterization gives significantly different values in the interactive model when compared to the values determined from the SHEBA data. This illustrates that the surface albedo parameterization with more complex dependence on surface features can give a degraded simulation of surface albedo if the simulation of surface features is deficient. The simulated snow melts too rapidly during spring using the SHCE parameterization and is too slow to accumulate during autumn. Problems with melting snow in part reflect that the modeled melting snow albedo is too low. The simulated pond fraction is too small and the pond depth too shallow for both simulations, because of the nocturnal freezing of ponds which appears to arise from not allowing ponds to warm above the freezing temperature.

The importance of spectral radiative interactions with the sea ice was shown by comparing the simulations with the SHCE and PW79 surface albedo parameterizations. Because PW79 specifies a broadband albedo, while the SHCE parameterization is spectral, significantly more shortwave radiation is transmitted to the ocean in the SHCE simulations since the visible radiation is able to penetrate the thin ice and enter the mixed layer. This results in a warmer ocean mixed layer for SHCE, which increases the lateral melting of leads (reflected by

the larger maximum lead fraction for SHCE) and also the amount of basal melting.

The different impacts of the two different surface albedo parameterizations were further emphasized by perturbation simulations using the single-cell ice thickness distribution model with each of the SHCE and PW79 parameterizations. These calculations illustrate that two different albedo parameterizations used in the same sea ice model, with the same average surface albedo and very nearly the same baseline conditions, can produce markedly different strengths of the ice-albedo feedback mechanism.

While it appears that a simple albedo parameterization tuned to give appropriate results for snow-covered and melting ice can give reasonable results when used in a sea ice model, it may be important to include a more complex albedo treatment to reproduce correctly the ice-albedo feedback and radiative interactions with the atmosphere. A more thorough assessment of whether an albedo parameterization of the complexity of SHCE is required for climate models requires feedback analysis done with a coupled ice/atmosphere model, and a concurrent assessment of the impact of other parameterizations in the sea ice model on the ice albedo feedback (e.g., snow cover and depth, ice thickness, melt ponds). To produce the correct spectral interactions with the atmosphere and changing cloud conditions, discrimination between diffuse and direct albedos is required. The feedback gain ratio is a useful metric for comparing parameterizations.

How representative is the SHEBA data set? SHEBA was characterized by relatively thin ice for a multiyear floe, and the melt season was about 25% longer than typical. In spite of these factors the albedos and their dependence on surface features and atmospheric conditions are believed to be typical of a relatively pristine multiyear ice floe. Fast ice in coastal regions may be associated with lower surface albedos [e.g., *Flato and Brown*, 1996]. Additionally, regions in the eastern Arctic may be exposed to more soot and sediment, which would lower the albedo. Further studies of albedo in the seasonal sea ice zone, coastal regions, and the eastern Arctic are needed to develop a basin-wide understanding of the albedo of the Arctic Ocean sea ice.

Acknowledgments. This research was supported by NSF SHEBA, NASA FIRE, and DOE ARM. We would like to thank C. Fairall and E. Andreas for making the surface flux data available to us, and we would also like to thank H. Stern for providing the ice deformation data for use in the model simulations. Comments on the manuscript from C. Bitz were very helpful.

References

Andreas, E.G., C.W. Fairall, P.S. Guest, and P.O.G. Persson, An overview of the SHEBA atmospheric surface flux program in *Fifth AMS Conference on Polar Meteroology and Oceanography*, pp.411-416, Am. Meteorol. Soc., Boston, Mass., 1999.

Barry, R. G., The parameterization of surface albedo for sea ice and its snow cover, *Prog. Phys. Geogr., 20*, 61-77, 1996.

Briegleb, B. P., and D. H. Bromwich, Polar radiation budgets of the NCAR CCM3, *J. Clim., 11*, 1246-1269, 1998.

Claffey, K. J., E. L. Andreas, D. K. Perovich, C. W. Fairall, P. S. Guest, and P. O. G. Persson, Surface temperature measurements at SHEBA, in *Fifth AMS Conference on Polar Meterology and Oceanography*, pp. 327-332, Am. Meteorol. Soc., Boston, Mass., 1999.

Curry, J. A., and P. J. Webster, *Thermodynamics of Atmospheres and Oceans*, Academic, San Diego, Calif., 465 pp., 1999.

Curry, J.A., J.L. Schramm, and E. E. Ebert, On the sea ice albedo climate feedback mechanism, *J. Clim., 8*, 240-247, 1995.

Curry, J.A., D. Randall, and W.B. Rossow, and J.L. Schramm, Overview of arctic cloud and radiation characteristics, *J. Clim., 9*, 1731-1764, 1996.

Curry, J.A, et al., FIRE Arctic Clouds Experiment, *Bull. Am Meteorol. Soc., 81*, 5-30, 2000.

Dickinson, R. E., G. A. Meehl, and W. M. Washington, Ice-albedo feedback in a CO_2-doubling simulation, *Clim. Change, 10*, 241-248, 1987.

Flato, G. M., and R. D. Brown, Variability and climate sensitivity of landfast Arctic sea ice, *J. Geophys. Res., 101*, 25,767-25,777, 1996.

Grenfell, T. C., and G. A. Maykut, The optical properties of ice and snow in the Arctic Basin, *J. Glaciol., 18*, 445-463. 1977.

Grenfell, T. C., and D. K. Perovich, Spectral albedos of sea ice and incident solar irradiance in the southern Beaufort Sea, *J. Geophys. Res., 89*, 3573-3580, 1984.

Hibler, W. D., Modeling a variable thickness sea ice cover, *Mon. Weather Rev., 108*, 1943-1973, 1980.

Holland, M.M.and J.A. Curry, The role of different physical process in determining the interdecadal variability of arctic sea ice, *J. Clim., 12*, 3319-3330, 1999.

Ingram, W. J., C. A. Wilson, and J. F. B. Mitchell, Modeling climate change: An assessment of sea ice and surface albedo feedbacks, *J. Geophys. Res., 94*, 8609-8622, 1989.

(IPCC), *The IPCC Scientific Assessment*, edited by J.T. Houghton, G.J. Jenkins, and J.J. Ephraums, 365 pp., Cambridge Univ. Press, New York, 1990.

Manabe, S., and R. J. Stouffer, Sensitivity of a global climate model to an increase of CO_2 concentration in the atmosphere, *J. Geophys. Res., 85*, 5529-5554, 1980.

Manabe, S., M. J. Spellman, and R. J. Stouffer, Transient responses of a coupled ocean-atmosphere model to gradual changes of atmospheric CO_2, II, Seasonal response, *J. Clim., 5*, 105-126, 1992.

Maykut, G.A., T.C. Grenfell, and W.F. Weeks, On estimating spatial and temporal variations in the properties of ice in the polar oceans, *J. Mar. Syst., 3*, 41-72, 1992.

Parkinson, C.L., and W.M. Washington, A large-scale numerical model of sea ice, *J. Geophys. Res., 84*, 311-337, 1979.

Perovich, D.K., *The Optical Properties of Sea Ice, CRREL Monogr. Ser. 96-1*, 25 pp., Cold Reg. Res. and Eng. Lab., Hanover, N.H., 1996.

Perovich, D. K., et al., Year on ice gives climate insights, *Eos Trans. AGU, 80*, 481, 1999.

Perovich, D.K., T.C. Grenfell, B. Light, J.A. Richter-Menge, W.B. Tucker III, and G.A. Maykut, The seasonal evolution of Arctic sea ice albedo, *J. Geophys. Res*, in press, 1999.

Ross, B., and J. E. Walsh, A comparison of simulated and observed fluctuations in summertime Arctic surface albedo, *J. Geophys. Res., 92*, 13,115-13,125, 1987.

Rossow, W. B., L. C. Garder, and A. A. Lacis, Global, seasonal cloud variations from satellite radiance measurements, part 1, Sensitivity of analysis, *J. Clim., 2*, 419-458, 1989.

Scharfen, G., R. G. Barry, D. A. Robinson, G. Kukla, and M. C. Serreze, Large-scale patterns of snow melt on Arctic sea ice mapped from meteorological satellite imagery, *Ann. Glaciol., 9*, 1-6, 1987.

Schramm, J. L., M. M Holland, and J. A. Curry, Modeling the thermodynamics of a sea ice thickness distribution, 1, Sensitivity to ice thickness resolution, *J. Geophys. Res., 102*, 23,079-23,091, 1997.

Spelman, M. J., and S. Manabe, Influence of oceanic heat transport upon the sensitivity of a model climate, *J. Geophys. Res., 89*, 571-586, 1984.

Tschudi, M., J.A. Curry, and J.M. Maslanik, Airborne observations of summertime surface features and their effect on surface albedo during SHEBA,. *J. Geophys. Res.*, in press, 2000.

Washington, W. W., and G. A. Meehl, General circulation model CO_2 sensitivity experiments: Snow-sea ice albedo parameterizations and globally averaged surface air temperature, *Clim. Change, 8*, 231-241, 1986.

J. A. Curry, J. O. Pinto, and J. L. Schramm, Department of Aerospace Engineering Sciences, University of Colorado, Campus Box 429, Boulder, CO 80309-0429. (curryja@cloud.colorado.edu; pinto@monsoon.colorado.edu; schramm@ucar.edu)

D. K. Perovich, U.S. Army Cold Regions Research and Engineering Laboratory, Hanover, NH 03755.

(Received December 14, 1999; revised April 11, 2000; accepted April 17, 2000.)